LASER INTERFEROMETER GRAVITATIONAL WAVE OBSERVATORY
- LIGO -
CALIFORNIA INSTITUTE OF TECHNOLOGY
MASSACHUSETTS INSTITUTE OF TECHNOLOGY

| **Document Type** | 2017/10/30 |
|---|---|
| **Characterization of the Signal Recycling Mirror Thermal Actuator for Active Mode Matching** | |
| Jonathan Richardson | |

*Distribution of this draft:*

All


**California Institute of Technology**
**LIGO Project - MS 51-33**
**Pasadena CA 91125**
Phone (626) 395-2129
Fax (626) 304-9834
E-mail: info@ligo.caltech.edu

**Massachusetts Institute of Technology**
**LIGO Project - MS NW22-295**
**Cambridge, MA 01239**
Phone (617) 253-4824
Fax (617) 253-7014
E-mail: info@ligo.mit.edu

WWW: http://www.ligo.caltech.edu/



Processed with LaTeX on 2017/10/30

**Abstract**

This note reports on characterization measurements of the thermal actuator proposed for the signal recycling mirrors (SRMs) in O3 for active mode matching. A mock $CO_2$ projector is constructed which provides a $10.2\ \mu$m heating beam of up to 310 mW incident on an SRM-like test optic. A co-aligned 633 nm probe beam and Hartmann wavefront sensor measure the resulting thermal lens. The actuator is demonstrated have a dynamic range of 16 mD in lens power, short of the theoretical expectation, but with strong linearity in applied heating power and high spherical mode purity. The power loss into higher-order spatial modes is found to be $< 0.25\%$ across the entire actuation range, meeting the low-loss requirement. Possible sources of the discrepancy in dynamic range are discussed, and it is argued that, even in the current configuration, the 50 mD target range is easily achievable by upgrading from a 400 mW to 1 W $CO_2$ laser.

# Contents

**1 Introduction** **3**

**2 Thermal Actuator Mock-Up** **3**

**3 Actuator Characterization** **3**
- 3.1 Methodology . . . . . 3
- 3.2 Dynamic Range . . . . . 4
- 3.3 Higher-Order Mode Losses . . . . . 4
- 3.4 Front Surface Thermo-Elastic Distortion . . . . . 4

**4 Discussion** **4**

# 1 Introduction

Achieving full sensitivity gains from squeezed light in Advanced LIGO requires mode matching to a finer precision than the specified tolerance ranges of radii of curvature of the optics allow. The static mismatches in radii of curvature can be corrected by thermally actuating certain optics. To actively match the laser mode exiting the interferometer to the output mode cleaner, a 400 mW $CO_2$ laser is proposed to provide a heating beam incident on the back surface of the signal recycling mirror (SRM), outside the signal recycling cavity. The heating beam creates a radial temperature gradient inside the SRM substrate, forming a thermo-refractive lens whose radius of curvature (ROC) can be finely controlled.

This note characterizes the performance of the proposed SRM thermal actuator. A mock $CO_2$ projector is constructed at Caltech which provides a $10.2$ $\mu$m heating beam of up to 310 mW incident on a test optic. A coaligned 633 nm probe beam and Hartmann wavefront sensor are used to profile the resulting thermal lens. This setup tests the three main requirements of an SRM actuator:

1. High dynamic range
2. High spherical mode purity
3. Low front surface thermo-elastic distortion

An estimated dynamic range of 50 mD is needed to fully span the possible range of static ROC mismatches. The $CO_2$ projector must also actuate very purely the spherical (TEM00) spatial mode, as any power transferred into high-order modes is filtered by the output mode cleaner (OMC) and converted directly into optical loss. Finally, the front surface (interferometer-facing side) of the SRM must exhibit low thermo-elastic distortion. When this condition is true, the $CO_2$ projector actuates purely the mode exiting the interferometer, without affecting the internal mode matching of the interferometer cavities.

In its current, power-limited configuration, the test actuator is demonstrated have a dynamic range of 16 mD in lens power, with high spatial mode purity. The power loss into higher-order spatial modes is found to be $< 0.25\%$ across the entire actuation range. Relative intensity noise of the $CO_2$ laser, $5\%$ at operating powers of $< 100$ mW and $10\%$ at higher power, dominates the error budget and could likely be improved with thermal stabilization. The optical setup is described further in §2, followed by the thermal lensing measurements obtained from it in §3. Finally, the results are compared to the theoretical lensing expectation in §4.

# 2 Thermal Actuator Mock-Up

Figure 1 shows the optical layout of the mock SRM thermal actuator. A heating beam provided by a $10.2$ $\mu$m adjustable-power Access Laser Company RF4 $CO_2$ laser is focused to 8 mm in diameter and directed onto the back surface of a 2" test optic at $25°$ incidence. The $CO_2$ projector can deliver a heating beam of up to 310 mW, limited by $10\%$ transmission losses on the table, and its power can be finely controlled. The test optic substrate, UV-grade fused silica, is chosen to match that of the in-situ SRM. Both optical surfaces are anti-reflection (AR) coated for 1.0-1.7 $\mu$m.

A 633 nm probe beam emitted by a superluminescent diode (SLED) is collimated to 4 mm in diameter and directed onto the front surface of the test optic, coaligned with the $10.2$ $\mu$m heating beam. The probe beam transmits through the optic and is lensed by the thermo-refractive gradient across the substrate. This lensing is measured by a Dalsa DS-22-01M60-11E Hartmann wavefront sensor (HWS) located 10 cm behind the test optic. The HWS is sensitive to sub-nm optical path differences (OPD) across the wavefront.

# 3 Actuator Characterization

## 3.1 Methodology

The degree and character of thermal lensing is inferred from OPD measurements using the overlap-integral method of Arain et al. (2006). In this method, the OPD change across the probe beam profile,

$s(x, y)$, is convolved with each transverse electromagnetic (TEM) spatial mode to characterize the geometry of the lensing medium. The lens component in the TEM00 (spherical) spatial mode is given by

$$I_{00} = \left| \frac{2}{\pi w^2} \int_x dx \int_y dy \, e^{-2(x^2+y^2)/w^2} \, e^{-4\pi i \left[s(x+x_0, y+y_0) - \frac{1}{2} S(x^2+y^2)\right]/\lambda} \right|^2 \quad (1)$$

where $\lambda = 633$ nm is the wavelength of the probe beam, $w = 2$ mm is its radius at the test optic, and $x_0$ and $y_0$ are the coordinates of its centroid. The lens power, or defocus, $S$, of the lensing medium is a free parameter fitted to maximize the overlap integral. The integral is normalized such that for a pure spherical lens, $I_{00} = 1$.

Figure 2 shows the overlap integral (eq. 1) evaluated at several levels of incident heating beam power. In each case, the true lens power is identified as the $S$-value which maximizes $I_{00}$. The maximum $I_{00}$ value is the spherical-mode lens component, while the residual deviation from unity, $1 - I_{00}$, represents the fraction of optical power transferred into higher-order spatial modes, becoming losses. These properties are analyzed further in the following sections.

### 3.2 Dynamic Range

Thermal lensing of the test optic is measured at a series of incident heating beam powers to determine the range of actuation and to verify the linearity of the process. Figure 3, top panel, shows the optical power of the induced lens as a function of applied heating. The error bars on the measurements are dominated by the intensity noise of the $CO_2$ laser, which is $5\%$ at low operating power ($< 100$ mW) and increases to $10\%$ at higher power. The lens power is confirmed to scale highly linearly with heating, as indicated by the two-parameter linear fit depicted by the green trace. The bottom panel shows the ROC, defined as the inverse of the lens power shown in the top panel. At the maximum incident heating beam power of 310 mW, a thermal lens with optical power +16 mD, or ROC 63 m, is measured to form. The agreement of the measured lensing with the theoretical expection is discussed in §4.

### 3.3 Higher-Order Mode Losses

As discussed in §3.1, the difference in the spherical-mode overlap integral (eq. 1) from unity, $1 - I_{00}$, reflects the fractional power loss into higher-order modes. Figure 2 shows this loss at several incident heating beam powers. In all cases it is found to be $< 0.25\%$, indicating high spherical mode purity across the entire range of actuation.

As a consistency check, Figure 4 shows the residual higher-order mode content at maximum incident heating power (310 mW). The left panel shows the measured OPD across the wavefront, while the right panel shows the residual after the spherical-mode term

$$s_{\rm fit}(x, y) = -\frac{1}{2} S \left[(x - x_0)^2 + (y - y_0)^2\right] \quad (2)$$

is subtracted. The OPD residual is in the range $\pm 5$ nm inside the 2 mm radius of the probe beam, indicating cancellation to better than $5\%$ of the peak OPD across the wavefront.

### 3.4 Front Surface Thermo-Elastic Distortion

[Still to be measured. An optical path is already set up to route the reflected probe beam from the front surface of the test optic onto the Hartmann sensor. This beam will sense purely the front surface thermo-elastic deformation, as the front and back surfaces are wedged $0.5°$ (no superposing of internal reflections).]

## 4 Discussion

The preceding measurements demonstrate that the thermal lens generated by the $CO_2$ projector scales linearly with applied heating, as expected, and has high spherical (TEM00) mode purity, with higher-order mode losses $< 0.25\%$. However, the achieved dynamic range of 16 mD fails to saturate the

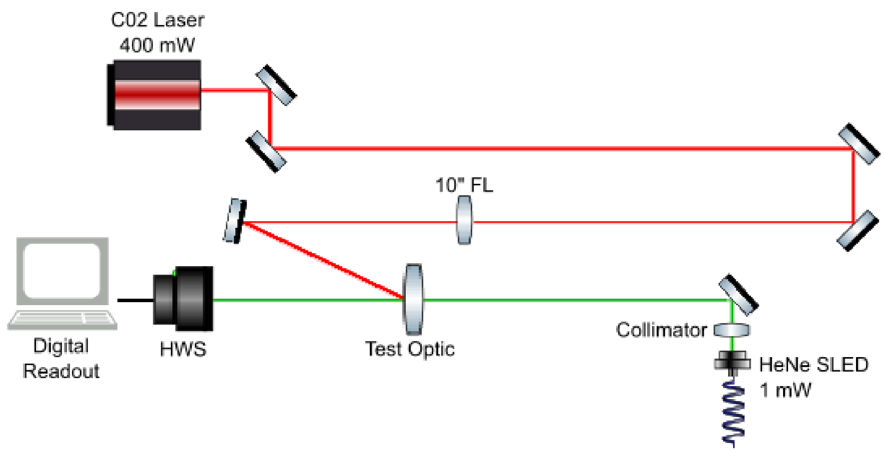


Figure 1: Layout of the $CO_2$ projector and wavefront sensing optics.

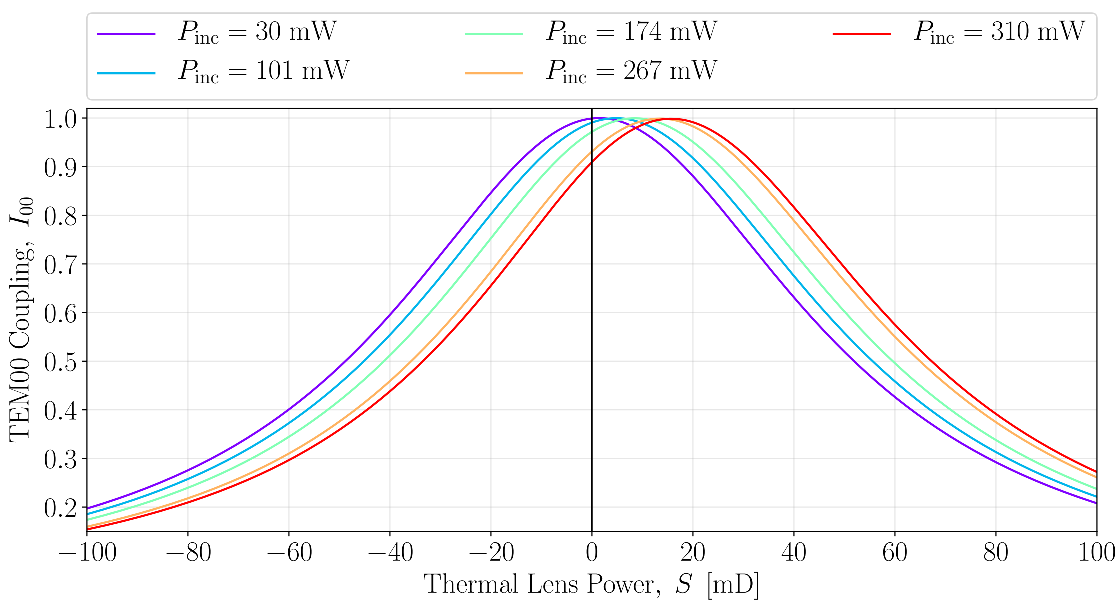


Figure 2: Overlap integral of the wavefront distortion with the TEM00 (spherical) spatial mode, measured at varying levels of incident heating beam power. The lens power, or defocus, of the lensing medium is identified as the $S$-value which maximizes the spherical-mode overlap. The fractional power loss into higher-order modes is given by $1 - I_{00}$.

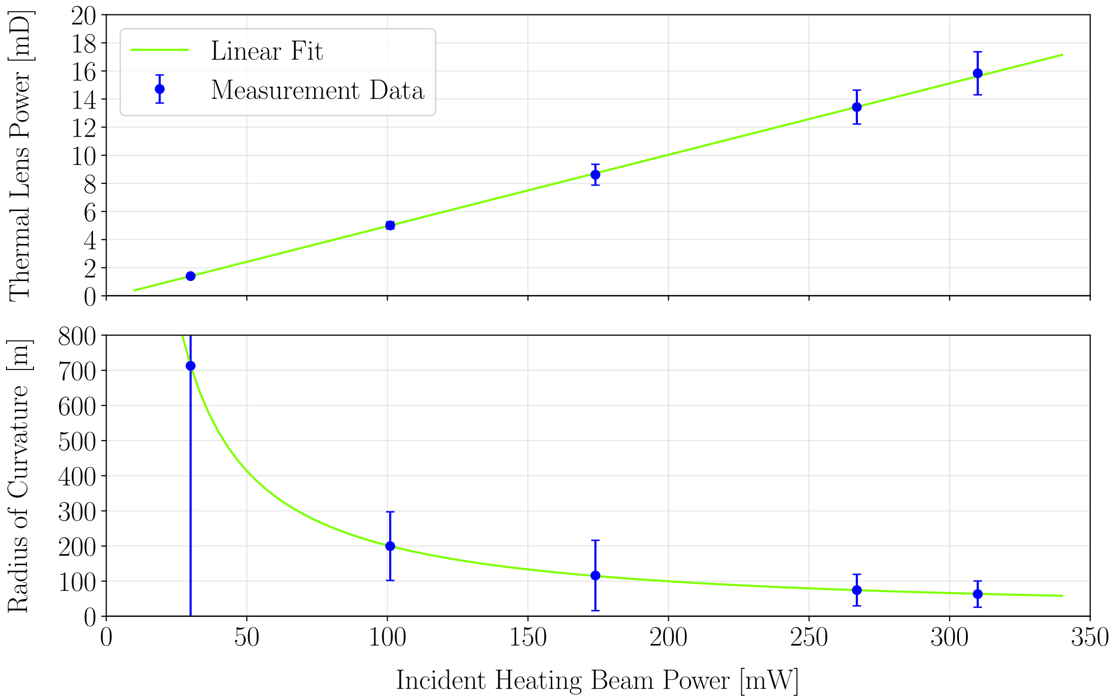


Figure 3: Thermal lensing measured as a function of applied heating beam power. Top: The optical power (defocus) of the lensing medium. Blue points are measurement data and the green curve is a two-parameter linear fit. Bottom: The radius of curvature (ROC), defined as the inverse of the defocus.

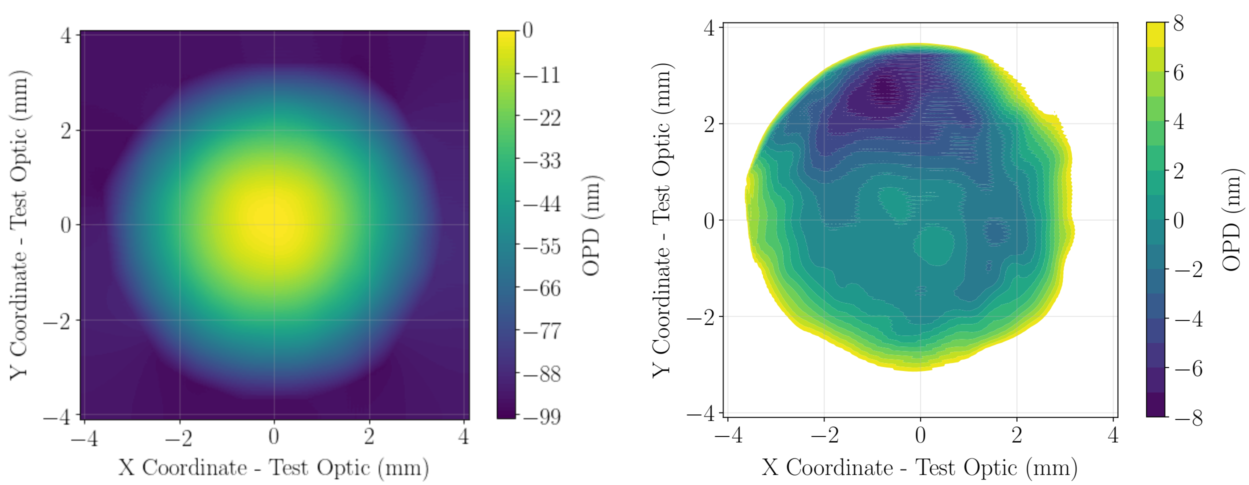


Figure 4: Left: OPD measurement across the probe beam wavefront, at maximum heating power (310 mW). Right: OPD residual after subtraction of the best-fit spherical-mode term. Cancellation to better than 5% of the peak OPD occurs inside the 2 mm probe beam radius, indicating high spherical mode purity of the thermal lens.

theoretical prediction by a significant factor. The thermal lens power is expected to follow

$$S = \frac{\beta}{\kappa} \frac{P_{\rm inc}}{\pi w_{\rm inc}^2} \tag{3}$$

where $P_{\rm inc}$ is the incident heating beam power, $w_{\rm inc} = 4$ mm is its radius, and $\beta = 8.6 \times 10^{-6}\ \rm K^{-1}$ and $\kappa = 1.38\ \rm W\ m^{-1}\ K^{-1}$ are the thermo-optic and thermal conductivity coefficients of fused silica, respectively. At the maximum deliverable heating beam power of 310 mW, the lens power is predicted to be 38 mD, more than twice the range actually achieved.

Several possibilities might explain this discrepancy. If the radius of the $CO_2$ heating beam is actually 6 mm instead of 4 mm, this would lower the theoretical prediction into agreement with the observed lens power. However, multiple occlusion measurements of the heating beam radius using a razor blade mounted on a micrometer stage disfavor this scenario. These measurements are noisy due to $\sim 10\%$ drift in the laser intensity over the measurement time scale, but they consistently favor a radius no larger than 4 mm.

Another possibility is that not all the heating power delivered to the test optic is reaching the substrate. Both sides of the test optic are AR-coated by Thorlabs for 1.0-1.7 $\mu$m. The vendor has only measured the performance of this coating to a maximum wavelength of 2 $\mu$m, at which point the reflectance is rapidly increasing. If a significant fraction of the 10 $\mu$m beam power is, in fact, back-scattered by the back surface coating, this too would explain the discrepancy. In this case, the effect of the 1 $\mu$m coating is likely a significant factor for the in-situ SRM as well.

Efforts to identify the source of disgreement between expected and achieved lens power are ongoing. Despite this discrepancy, the demonstrated strong linearity of the lensing as a function of heating power (see Figure 3) suggests that the required dynamic range could be easily achieved, even in the current optical configuration, by upgrading the $CO_2$ laser from 400 mW to 1 W.